Physica B 404 (2009) 3167–3171

Contents lists available at ScienceDirect

Physica B

journal homepage: www.elsevier.com/locate/physb

Energy-resolved spatial inhomogeneity of disordered Mott systems

E.C. Andrade [a,b], E. Miranda [b], V. Dobrosavljević [a,*]

[a] Department of Physics and National High Magnetic Field Laboratory, Florida State University, Tallahassee, FL 32306, USA
[b] Instituto de Física Gleb Wataghin, Unicamp, C.P. 6165, Campinas, SP 13083-970, Brazil

ARTICLE INFO

PACS:
71.10.Fd
71.30.+h
71.23.−k
71.10.Hf

Keywords:
Mott transition
Disorder
Non-Fermi liquid
Griffiths phase

ABSTRACT

We investigate the effects of weak to moderate disorder on the $T = 0$ Mott metal–insulator transition in two dimensions. Our model calculations demonstrate that the electronic states close to the Fermi energy become more spatially homogeneous in the critical region. Remarkably, the higher energy states show the opposite behavior: they display enhanced spatial inhomogeneity precisely in the close vicinity to the Mott transition. We suggest that such energy-resolved disorder screening is a generic property of disordered Mott systems.

1. Introduction

The observation of a metal–insulator transition in high-mobility 2d electron systems at zero magnetic field has sparked renewed interest in this type of transition [1]. In these systems, electron–electron interactions represent the largest energy scale in the problem [1]. Further evidence for the crucial role of electronic correlations has come from complementary experiments [2,3] reporting a substantial mass enhancement close to the metal–insulator transition. Taken together, these experimental results stress the importance of the ill-understood effects of disorder in strongly correlated electronic systems [4].

In one of the first studies of its kind, Tanasković et al. have investigated the interplay of strong correlations and disorder using a dynamical mean-field theory (DMFT) [5] approach [6]. The DMFT approach to disordered systems treats correlations on a local level by solving the embedded-atom strongly correlated Anderson impurity problem in the self-consistently determined *fixed* bath of the other electrons. One is thus forced to consider an *ensemble* of single-impurity actions, one for each lattice site. Remarkably, Tanasković et al. found that very strong site disorder screening emerges precisely in the vicinity of the Mott metal–insulator transition [7]. This effect can be traced back to the pinning of the single-impurity Kondo resonances to the Fermi level, which acts to suppress the effective randomness.

Motivated by this striking result, we extended their work to finite dimensions. To treat both strong correlations and disorder in a non-perturbative fashion at $T = 0$, we use a generalization of the DMFT, the statistical DMFT (*statDMFT*) [8], implemented using a slave boson impurity solver [9]. This approach is equivalent to the description of the effects of disorder through a Gutzwiller-type wave function [10,11], which in the clean case realizes the Brinkman–Rice scenario of the Mott transition [12]. The statDMFT method retains the local treatment of electronic correlations. However, in contrast to the infinite-dimensional DMFT approach, here each strongly correlated site sees a *different bath of electrons*, reflecting the strong spatial fluctuations of their immediate environment. We find that, concomitant to a strong pinning effect, additional effective disorder is also generated through an increasingly broader distribution of quasi-particle weights. Their interplay leads to a non-trivial landscape in energy space: the proximity to the Mott transition acts to suppress density of states fluctuations close to the Fermi level, while at the same time *enhancing* them at higher energies.

2. Strongly correlated theory

We focus on the disordered Hubbard model

$$H = \sum_{i,\sigma} \varepsilon_i c^\dagger_{i\sigma} c_{i\sigma} - t \sum_{\langle ij \rangle,\sigma} (c^\dagger_{i\sigma} c_{j\sigma} + \text{h.c.}) + U \sum_i n_{i\uparrow} n_{i\downarrow}, \quad (1)$$

where $c^\dagger_{i\sigma}(c_{i\sigma})$ is the creation (annihilation) operator of electrons with spin projection σ on site i, is the nearest-neighbor hopping amplitude, U is the on-site Hubbard repulsion, $n_{i\sigma} = c^\dagger_{i\sigma} c_{i\sigma}$ is the

* Corresponding author. Tel.: +1 850 644 5693.
E-mail address: vlad@magnet.fsu.edu (V. Dobrosavljević).

0921-4526/$ - see front matter © 2009 Elsevier B.V. All rights reserved.
doi:10.1016/j.physb.2009.07.056

number operator, and the site energies ε_i are uniformly distributed in the interval $[-W/2, W/2]$, where W is the disorder strength. We work at half filling (chemical potential $\mu = U/2$) on an $L \times L$ square lattice with periodic boundary conditions. All energies will be expressed in units of the clean Fermi energy (the half-bandwidth D) $E_F = 4t$.

We treat the Hamiltonian of Eq. (1) in its paramagnetic phase within the statDMFT [8]. This theory is exact in the non-interacting limit and reduces to the standard DMFT in the absence of disorder. Unlike the DMFT, however, it incorporates Anderson localization effects. We start by writing an effective action (in imaginary time) for a given site i, with the simplification that we neglect all non-quadratic terms in the local fermionic operators except for the local U-term

$$S_{eff}^{(i)} = \sum_{\sigma} \int_0^{\beta} d\tau c_{i\sigma}^{\dagger}(\tau)(\partial_\tau + \varepsilon_i - \mu)c_{i\sigma}(\tau) + \sum_{\sigma} \int_0^{\beta} d\tau \int_0^{\beta} d\tau' c_{i\sigma}^{\dagger}(\tau)\Delta_i(\tau - \tau')c_{i\sigma}(\tau') + U \int_0^{\beta} d\tau n_{i\uparrow}(\tau)n_{i\downarrow}(\tau). \quad (2)$$

The site i is connected with the rest of the lattice through the bath (or "cavity") function $\Delta_i(\tau)$, which in statDMFT (but in contrast to DMFT) varies from site to site and thus exhibits strong spatial fluctuations.

The effective action in Eq. (2) is precisely the action of an Anderson impurity model [13] embedded in a sea of conduction electrons described by $\Delta_i(\tau)$. Therefore, this approach maps the original Hubbard Hamiltonian in Eq. (1) onto an *ensemble* of single-impurity Anderson Hamiltonians [14]. The local i-site Green's function, calculated under the dynamics dictated by the effective action in Eq. (2), can be written as ($i\omega$ is a Matsubara frequency)

$$G_i^{loc}(i\omega) = \frac{1}{i\omega + \mu - \varepsilon_i - \Sigma_i(i\omega) - \Delta_i(i\omega)}, \quad (3)$$

which also serves as a definition of $\Sigma_i(i\omega)$, the i-site self-energy. It is important to point out that within statDMFT the electronic self-energy $\Sigma_i(i\omega)$ is still local, albeit site-dependent.

The bath function $\Delta_i(i\omega)$ can be viewed as the Weiss field of this mean-field theory, here elevated to a full function of frequency or time. It is determined through a self-consistency condition that demands that the Green's function $G_i^{loc}(i\omega)$ obtained from the effective action in Eq. (2) be equal to the diagonal (local) part of the full lattice Green's function

$$G_{ii}(i\omega) = \left[\frac{1}{i\omega - \boldsymbol{\varepsilon} - \mathbf{H}_0 - \boldsymbol{\Sigma}(i\omega)}\right]_{ii}, \quad (4)$$

where $\boldsymbol{\Sigma}(i\omega)$ and $\boldsymbol{\varepsilon}$ are site-diagonal matrices $[\boldsymbol{\Sigma}(i\omega)]_{ij} = \Sigma_i(i\omega)\delta_{ij}$, $[\boldsymbol{\varepsilon}]_{ij} = \varepsilon_i\delta_{ij}$ and $\mathbf{H}_0$ is the clean ($W = 0$) and non-interacting ($U = 0$) lattice Hamiltonian. In general, this step involves the inversion of the frequency-dependent matrix within brackets in Eq. (4).

It is worthwhile to point out that the statDMFT approach requires a massive numerical effort since it is necessary to solve a single-impurity problem *for every lattice site* as well to perform the inversion implied by the self-consistency condition. On the other hand, it provides access to entire distribution functions and accounts for spatial correlations between local quantities.

To find $\Sigma_i(i\omega)$, we need to solve the auxiliary single impurity problems for a given set of $\Delta_i(i\omega)$. For this task, we have used the four-boson mean-field theory of Kotliar and Ruckenstein [9] at $T = 0$, which is equivalent to the well-known Gutzwiller variational approximation. In practice, we need to solve a pair of non-linear equations for the site-dependent Kotliar–Ruckenstein slave boson amplitudes e_i and d_i [9,6]

$$2\int_{-\infty}^{\infty} \frac{d\omega}{2\pi} G_i^{loc}(i\omega) = Z_i(1 - e_i^2 + d_i^2), \quad (5)$$

$$\int_{-\infty}^{\infty} \frac{d\omega}{2\pi} \Delta_i(i\omega)G_i^{loc}(i\omega) = \frac{Z_i e_i(\varepsilon_i - Z_i\nu_i - \mu)}{\partial Z_i/\partial e_i}, \quad (6)$$

where

$$Z_i = \frac{2(e_i + d_i)^2(1 - e_i^2 - d_i^2)}{1 - (e_i^2 - d_i^2)^2}, \quad (7)$$

and

$$Z_i\nu_i = \varepsilon_i - \mu + \frac{Ud_i}{\left(\frac{\partial Z_i}{\partial e_i}d_i + \frac{\partial Z_i}{\partial d_i}e_i\right)}\frac{\partial Z_i}{\partial e_i}. \quad (8)$$

Eqs. (5)–(6) involve the local i-site Green's function $G_i^{loc}(i\omega)$. In the Kotliar–Ruckenstein theory, the i-site self-energy $\Sigma_i(i\omega)$ is given by

$$\Sigma_i(i\omega) = (1 - Z_i^{-1})i\omega + \nu_i - \varepsilon_i + \mu, \quad (9)$$

which, when plugged into Eq. (3) yields

$$G_i^{loc}(i\omega) = \frac{Z_i}{i\omega - Z_i\nu_i - Z_i\Delta_i(i\omega)}. \quad (10)$$

It is clear that Z_i has the physical interpretation of a quasi-particle weight (wave function renormalization). It also renormalizes the hybridization function, thus setting the local Kondo temperature [15–17]. Furthermore, from Eq. (9) we see that ν_i can be viewed as a renormalized on-site disorder potential

$$\nu_i = \varepsilon_i + \Sigma_i(0) - \mu. \quad (11)$$

We numerically solved the disordered Hubbard model with statDMFT, using the Kotliar–Ruckenstein theory as the impurity solver, for several lattice sizes up to $L = 50$. For every (U, W) pair we typically generated around forty realizations of disorder. We carefully verified that for such large lattices, all our results are robust and essentially independent of the system size (see, e.g., the inset of Fig. 3).

3. The disordered Mott transition

According to the scaling theory of localization, any amount of disorder drives a system with dimension equal to or smaller than two to an insulating phase [18]. However, this result was obtained in the absence of electron–electron interactions. In the last few years, strong numerical evidence has been obtained indicating that interactions can act to enhance the conducting properties of 2d electronic systems [19–21]. Moreover, the stability of a 2d metal with respect to weak-localization corrections has been investigated by Punnoose and Finkelstein [22] in very careful recent work. These authors have demonstrated that any 2d metal remains stable with respect to sufficiently weak disorder due to additional (anti-localizing) interaction corrections. Note, however, that both the weak-localization and the corresponding interaction corrections are manifested only through a very weak, logarithmic dependence on the system size. Such subtle finite size effects are not visible for the very weak (renormalized) disorder we deal with in this work. Nevertheless, based on the very convincing considerations of Punnoose and Finkelstein, the stability of a 2d metal is beyond immediate doubt and these issues are not of relevance for the questions we focus on in this paper.

The low energy behavior on the metallic side of the transition is characterized by the distribution of the local quasi-particle

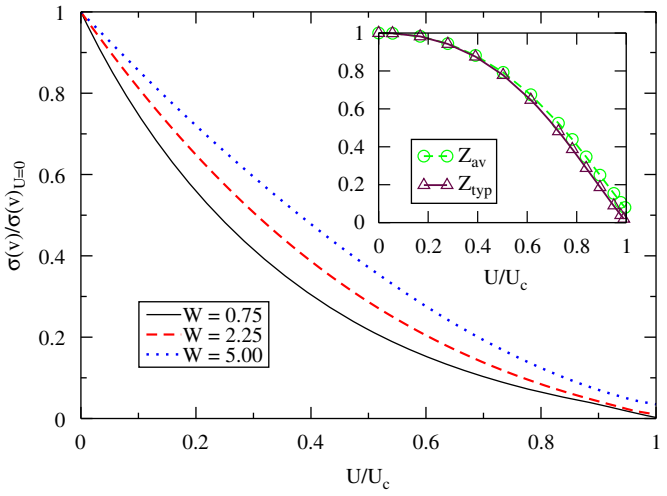

Fig. 1. Strength of the renormalized site energy disorder, as given by the standard deviation $\sigma(\nu)$ of $P(\nu)$, normalized by its non-interacting value (see text for definition of ν). Close to the Mott transition, the disorder screening remains strong even for moderate values of disorder. Results are shown for $L = 20$. In the inset we show the typical (Z_{typ}) and average (Z_{av}) values of the local quasi-particle weight Z_i as functions of the interaction U. The Mott transition is identified by the vanishing of Z_{typ}. We note that Z_{av} is finite at U_c indicating that a fraction of the sites remains nearly empty or doubly occupied. Results are shown for $L = 20$ and $W = 2.25$.

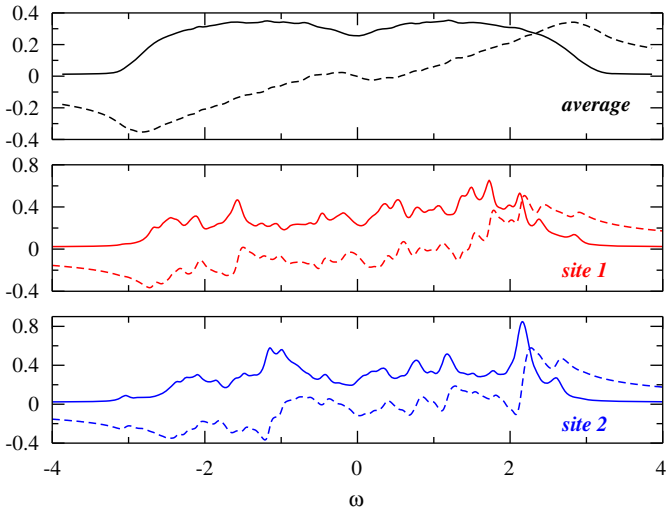

Fig. 2. Real (dashed lines) and imaginary (full lines) parts of the hybridization function $\Delta_i(\omega)$. Although the average value of $\Delta_i(\omega)$ is particle–hole symmetric, for an arbitrary site $\Delta_i(\omega)$ is locally particle–hole asymmetric. Results are shown for $L = 20$ and $W = U = 2.25$.

weight Z_i. Following previous studies of the disordered Mott transition [8,6,23], we choose the typical value of Z_i, here defined through the geometrical average $Z_{typ} = \exp\{\langle \ln Z_i \rangle\}$, as the order parameter of the transition. This quantity vanishes linearly at a critical value of interaction $U_c \equiv U_c(W)$ at which the Mott transition takes place, marking the transmutation of most itinerant electrons into local magnetic moments (see the inset of Fig. 1). Because random site energies tend to push the local occupation away from half filling, $U_c(W)$ is an increasing function of the disorder strength W. A more complete discussion of the phase diagram can be found in Ref. [24]. We also stress that the average value of the quasi-particle weight Z_{av} is small yet finite at the Mott transition (inset of Fig. 1), indicating that some sites remain either empty ($e_i = 1$) or doubly occupied ($d_i = 1$) and do not give rise to localized magnetic moments.

4. Particle–hole symmetry and strong disorder screening

Using the fact that in the current statDMFT approach the lattice problem is mapped onto an *ensemble* of auxiliary Anderson impurity problems, we can characterize the approach to the Mott transition by a steady decrease of the local Kondo temperature T_K^i ($T_K^i \propto Z_i$). Moreover, the renormalized disorder potential ν_i can be thought of as the position of the local Kondo resonance energy.

In the DMFT limit ($d \to \infty$), each site has many neighbors and thus is embedded in the same (self-averaged) environment described by $\Delta_{av}(\omega)$. In this regime, as long as $\Delta_{av}(\omega)$ is particle–hole symmetric, we find *perfect* disorder screening close to the Mott transition [6]. This happens because, as we increase U towards $U_c(W)$, we approach the Kondo limit, $Z_i \to 0$, causing ν_i (the Kondo resonance) to be "pinned" to the Fermi energy [25].

However, within the *statDMFT* approach, $\Delta_i(\omega)$ fluctuates strongly from site-to-site and is not locally particle–hole symmetric (see Fig. 2). For this reason, we expect that ν_i will also have a contribution which is proportional to $\mathrm{Re}[\Delta_i(0)]$. Therefore, we have no guarantee that a similar mechanism of disorder screening will persist close to the critical point in 2d. Surprisingly, for small and moderate disorder ($W \lesssim U_c$), we do get a very strong disorder screening close to the Mott metal–insulator transition (see Figs. 1 and 3).

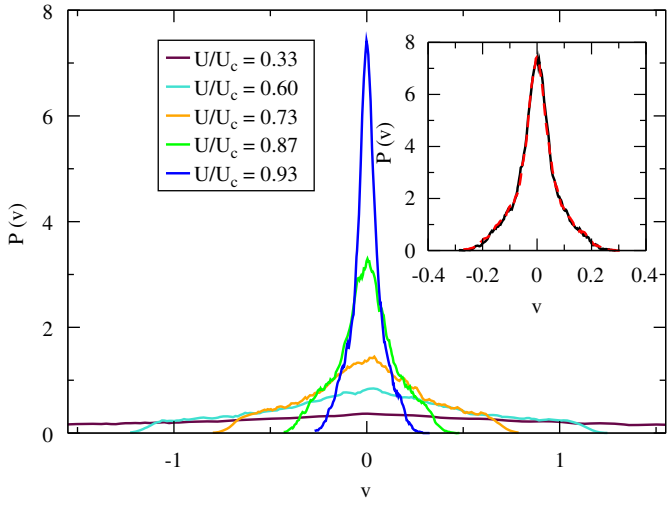

Fig. 3. Probability distribution function $P(\nu)$ of the renormalized site energy ν. As we move towards the Mott transition, disorder screening takes place and $P(\nu)$ becomes increasingly narrower. Results are shown for $L = 50$ and $W = 2.25$. The inset illustrates how for such large lattices our results for $P(\nu)$ are essentially independent of the system size: results are shown for $L = 20$, full line, and $L = 50$, dashed line at $W = 2.25$ and $U/U_c = 0.93$.

5. Mott droplets

The site-to-site fluctuations in the hybridization function encode *spatial correlations* between the physical quantities, implying, for example, that the value of the local quasi-particle weight at a given site depends on the quasi-particle weight values at the neighboring sites. Therefore, due to rare disorder configurations, it is possible to find regions containing sites in which $Z_i \ll Z_{typ}$ (red regions in Fig. 4). Since the approach to the Mott insulator corresponds to $Z \to 0$, such regions with $Z_i \ll Z_{typ}$ should be recognized as "almost localized" Mott droplets (consisting of

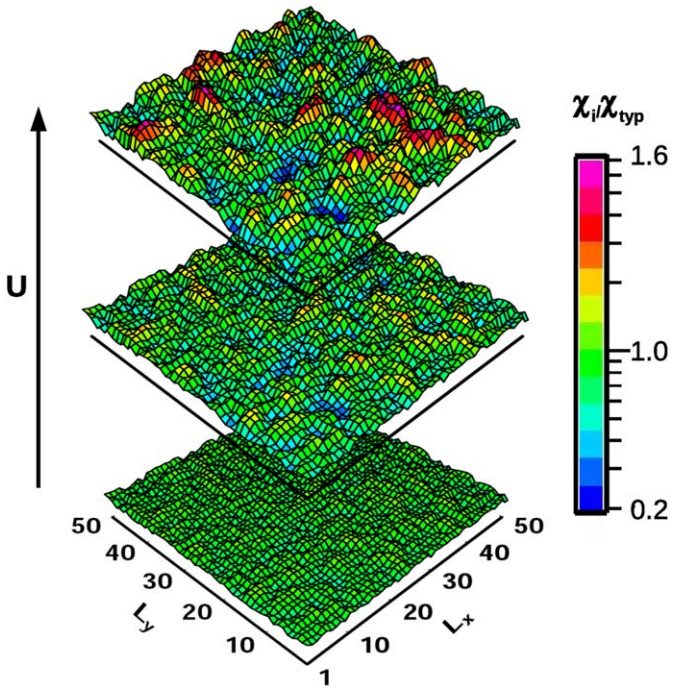

Fig. 4. Spatial distribution of the of the local susceptibility $\chi_i \sim Z_i^{-1}$ normalized by its typical value χ_{typ}. From bottom to the top we have $U/U_c = 0.73,\ 0.87,\ 0.96$. The color scale is logarithmic in order to stress that, as we approach the critical point, we have the formation of regions in which $\chi_i \gg \chi_{typ}$ (localized magnetic moments) and $\chi_i \ll \chi_{typ}$ (Anderson insulator droplets). Results are shown for $W = 2.25$ and $L = 50$.

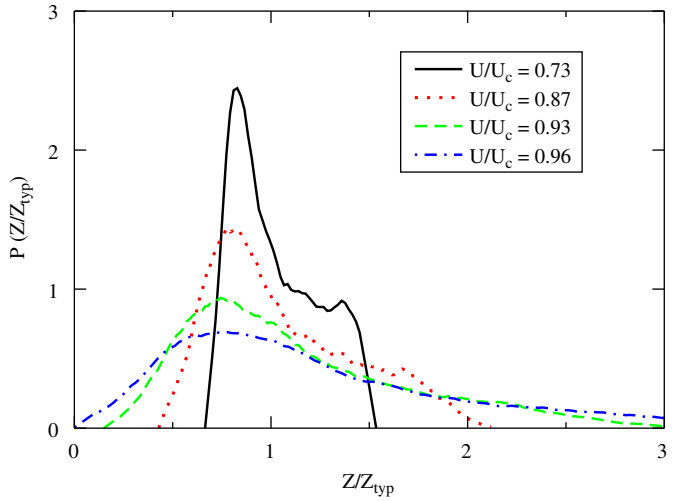

Fig. 5. Distribution of the quasi-particle weight divided by its typical value for $W = 2.25$ and $U_c(W) \simeq 3.7$. As we approach the critical point, $P(Z/Z_{typ})$ becomes increasingly broader, even though the bare disorder strength W is kept fixed. Results are shown for $L = 20$.

localized magnetic moments [26–28]) inside the strongly correlated metallic host. Within our Brinkman–Rice picture, each local region provides [8,12] a contribution $\chi_i \sim \gamma_i \sim Z_i^{-1}$ to the spin susceptibility or the Sommerfeld coefficient, respectively. The local regions with the smallest Z_i thus dominate the thermodynamic response and will ultimately give rise to an Electronic Griffiths Phase in the vicinity of the disordered Mott metal–insulator transition [24,29,30].

The Mott droplets have a direct influence on the probability distribution function $P(Z/Z_{typ})$, since they give rise to a low-Z tail, contributing to the fact that $P(Z/Z_{typ})$ actually broadens as we approach the Mott metal–insulator transition for a *fixed* W, as shown in Figs. 4 and 5.

Surely, there is also a contribution to the broadening of $P(Z/Z_{typ})$ coming from the high-Z tail originating from those sites with $Z_i \gg Z_{typ}$. Such sites retain a finite Z_i at the transition and are nearly empty or doubly occupied, giving rise to Anderson insulating regions (blue regions in Fig. 4). The coexistence of localized magnetic moments, and nearly empty or doubly occupied sites close to the critical point is characteristic of a two-fluid behavior, as discussed in Ref. [23]. Nevertheless, this interesting phenomenon is not relevant for the present analysis, since the major contribution to the energy-resolved inhomogeneities, discussed in the next section, as well as to the thermodynamic response, comes from the Mott droplets.

6. Energy-resolved inhomogeneities

From the above discussion, it is clear that the behaviors of $P(v)$ and $P(Z/Z_{typ})$ near the Mott metal–insulator transition are quite distinct. While the former exhibits strong disorder screening (Fig. 3), the latter suggests that the disorder is actually increasing (Fig. 5). This dichotomy gives rise to an *energy-dependent effective disorder*, which manifests itself, for example, in the spatial structure of the local density of states. The local density of states is defined as $\rho_i(\omega) = (1/\pi)\mathrm{Im}[G_{ii}(\omega - i0^+)]$, where the lattice Green's function was given in Eq. (4), and has the following expression within our Brinkman–Rice picture

$$G_{ii}(\omega) = \left[\frac{1}{\mathbf{Z}^{-1}\omega - \mathbf{v} - \mathbf{H}_0}\right]_{ii}, \tag{12}$$

where $\mathbf{Z}$ and $\mathbf{v}$ are site-diagonal matrices such that $[\mathbf{Z}]_{ij} = Z_i\delta_{ij}$, $[\mathbf{v}]_{ij} = v_i\delta_{ij}$. Therefore, the frequency-dependent effective disorder potential "seen" by the quasi-particles at energy ω can be defined as

$$\varepsilon_i^{eff}(\omega) = v_i - \frac{\omega}{Z_i}. \tag{13}$$

In our Brinkman–Rice scenario of the Mott transition, the quasi-particle bandwidth is reduced by Z_{typ} as $U \to U_c$. To monitor the behavior within the quasi-particle band, we therefore introduce a rescaled frequency $\omega^* = \omega/Z_{typ}$, which we will keep constant as we approach the transition. In Fig. 6, we show topographic maps of the local density of states for one specific realization of disorder. Because of strong disorder screening, $v_i \approx 0$ close to the critical point. Thus, if the system is examined at the Fermi energy ($\omega = 0$), it becomes more and more homogeneous as the transition is approached. At higher energies ($\omega^* \neq 0$), however, the fluctuations in Z_{typ}/Z_i come into play. Since they are very pronounced close to the Mott transition, we instead find a strong enhancement of the spatial inhomogeneity.

This result is surprisingly reminiscent of recent spectroscopic images on doped cuprates [31]. Our theory, which focuses on local (Kondo-like) effects of strong correlations (while neglecting inter-site magnetic correlations) and does not include any physics associated with superconducting pairing, strongly suggests that such energy-resolved inhomogeneity is a robust and general feature of disordered Mott systems. Indeed, recent results corroborate this picture of an energy-resolved strong-correlation driven disorder screening [32].

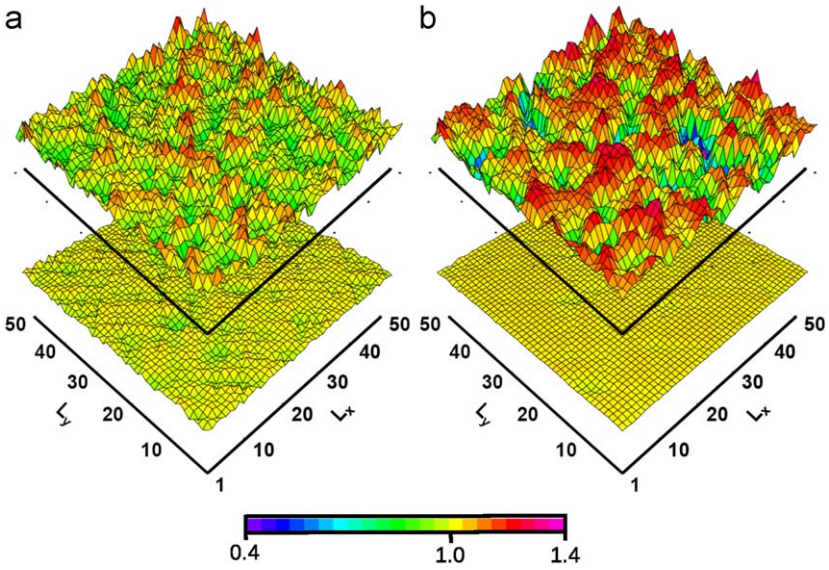

Fig. 6. Spatial distribution of the local density of states normalized by its clean and non-interacting value for one given realization of disorder and two distinct values of interaction: (a) $U/U_c = 0.87$ and (b) $U/U_c = 0.96$, where $U_c \simeq 3.7$. We have $\omega = 0$ in the bottom figures and $\omega/Z_{typ} = 0.1$ in the top ones. At the Fermi energy, the local density of states distribution becomes homogeneous as we approach the Mott transition. Conversely, if we move even slightly away from the Fermi energy, the distribution becomes in fact more inhomogeneous close to U_c. Results are shown for $L = 50$ and $W = 2.25$.

7. Conclusions

We have discussed the results of a Brinkman–Rice approach to the disordered Mott transition. A striking feature that is apparent in this scenario is the different behaviors of the effective site disorder and the quasi-particle weights as the transition is approached. Whereas randomness in the former is suppressed, the latter becomes extremely singular and broad on the way to the Mott insulator. The end result of this dichotomy is a non-trivial energy-space landscape, which is signaled by an energy-dependent inhomogeneity.

Acknowledgments

This work was supported by FAPESP through Grants 04/12098-6 (ECA) and 07/57630-5 (EM), CAPES through Grant 1455/07-9 (ECA), CNPq through Grant 305227/2007-6 (EM), and by NSF through Grant DMR-0542026 (VD).

References

[1] E. Abrahams, S.V. Kravchenko, M.P. Sarachik, Rev. Mod. Phys. 73 (2001) 251.
[2] V.M. Pudalov, et al., Phys. Rev. Lett. 88 (2002) 196404.
[3] A.A. Shashkin, et al., Phys. Rev. B 66 (2002) 073303.
[4] P.A. Lee, T.V. Ramakrishnan, Rev. Mod. Phys. 57 (1985) 287.
[5] A. Georges, G. Kotliar, W. Krauth, M. Rozenberg, Rev. Mod. Phys. 68 (1996) 13.
[6] D. Tanasković, V. Dobrosavljević, E. Abrahams, G. Kotliar, Phys. Rev. Lett. 91 (2003) 066603.
[7] N.F. Mott, Metal–Insulator Transition, Taylor & Francis, London, 1990.
[8] V. Dobrosavljević, G. Kotliar, Phys. Rev. Lett. 78 (1997) 3943.
[9] G. Kotliar, A. Ruckenstein, Phys. Rev. Lett. 57 (1986) 1362.
[10] M.C. Gutzwiller, Phys. Rev. Lett. 10 (1963) 159.
[11] M.C. Gutzwiller, Phys. Rev. 137 (1965) A1726.
[12] W.F. Brinkman, T.M. Rice, Phys. Rev. B 2 (1970) 4302.
[13] P.W. Anderson, Phys. Rev. 124 (1961) 41.
[14] A. Georges, G. Kotliar, Phys. Rev. B 45 (1992) 6479.
[15] N. Read, D.M. Newns, J. Phys. C 16 (1983) 3273.
[16] N. Read, D.M. Newns, J. Phys. C 16 (1983) L1055.
[17] P. Coleman, Phys. Rev. B 35 (1987) 5072.
[18] E. Abrahams, P.W. Anderson, D.C. Licciardelo, T. Ramakrishnan, Phys. Rev. Lett. 42 (1979) 673.
[19] D. Heidarian, N. Trivedi, Phys. Rev. Lett. 93 (2004) 126401.
[20] P.B. Chakraborty, P.J.H. Denteneer, R.T. Scalettar, Phys. Rev. B 75 (2007) 125117.
[21] Y. Song, R. Wortis, W.A. Atkinson, Phys. Rev. B 77 (2008) 054202.
[22] A. Punnoose, A.M. Finkel'stein, Science 310 (2005) 289.
[23] M.C.O. Aguiar, V. Dobrosavljević, E. Abrahams, G. Kotliar, Phys. Rev. B 73 (2006) 115117.
[24] E.C. Andrade, E. Miranda, V. Dobrosavljević, Phys. Rev. Lett. 102 (2009) 206403.
[25] P. Nozières, J. Low Temp. Phys. 17 (1974) 31.
[26] M. Milovanović, S. Sachdev, R.N. Bhatt, Phys. Rev. Lett. 63 (1989) 82.
[27] M.A. Paalanen, J.E. Graebner, R.N. Bhatt, S. Sachdev, Phys. Rev. Lett. 61 (1988) 597.
[28] V. Dobrosavljević, G. Kotliar, Phys. Rev. Lett. 71 (1993) 3218.
[29] E. Miranda, V. Dobrosavljević, Rep. Progr. Phys. 68 (2005) 2337.
[30] T. Vojta, J. Phys. A 39 (2006) R143.
[31] K. McElroy, et al., Science 309 (2005) 1048.
[32] A. Garg, M. Randeria, N. Trivedi, Natur. Phys. 4 (2008) 762.